Activated Transport in Polymer Grafted Nanoparticle Melts

Mayank Jhalaria,[1] Yucheng Huang,[2] Eric Ruzicka,[2] Madhusudan Tyagi,[3,4] Reiner Zorn,[5] Michaela Zamponi,[6] Victoria García Sakai,[7] Brian C. Benicewicz,[2] Sanat K. Kumar*,[1]

[1]Department of Chemical Engineering, Columbia University, New York, NY, 10027

[2]Department of Chemistry and Biochemistry, University of South Carolina, Columbia, SC, 29208.

[3]NIST Center for Neutron Research, National Institute of Standards and Technology, Gaithersburg, Maryland 20899-6102, United States

[4]Department of Materials Science and Engineering, University of Maryland, College Park, MD 20742, United States

[5]Forschungszentrum Jülich GmbH, Jülich Centre for Neutron Science (JCNS-1) and

Institute for Biological Information Processing (IBI-8), 52425 Jülich, Germany

[6]Forschungszentrum Jülich GmbH, Jülich Centre for Neutron Science at MLZ, Lichtenbergstr. 1, 85748 Garching, Germany

[7]ISIS Neutron and Muon Source, Rutherford Appleton Laboratory, Chilton, Oxfordshire, OX11 0QX, UK

KEYWORDS: polymer brushes, quasielastic neutron scattering, facilitated transport, gas transport, polymer dynamics, segmental dynamics

ABSTRACT

We measure the activation energy for the local segmental dynamics of polymer chains densely grafted to nanoparticles (NPs) using quasielastic neutron scattering. We aim to understand the underpinning physics of the experimentally measured enhanced gas transport in polymer grafted nanoparticle (GNPs) based membranes relative to the neat polymer (without NPs), especially the permeability maximum which occurs at intermediate chain lengths. We find that the activation energy goes through a minimum function of chain length, while the elementary jump size goes through a maximum around the same chain length. These results, likely, are the dynamic consequence of a structural transition of the grafted polymer brush from "extended" to "interpenetrated" with increasing chain length at fixed grafting density. Evidently, the regimes of different graft chain lengths near this structural transition are associated with lower activation energy likely due to fluctuation effects which also leads to enhanced gas transport.

A key molecular mechanism for transport in a condensed polymer phase was proposed by Brandt[1] and Freeman,[2] who postulated that the activation energy, E_A, for diffusion depends on the penetrant's kinetic diameter, d:

$$E_A = cd^2 - f \quad (1)$$

This equation defines a parameter f which on its own has no physical interpretation. However, a characteristic size of the polymer free volume[3-5] can be defined as $d_0 = \sqrt{f/c}$ (where c is the apparent stiffness of the medium). While the free volume is an easy metric to describe and measure (e.g., using positron annihilation lifetime spectroscopy, PALS),[6, 7] it is difficult to understand, relate to the molecular details defining the medium and hence to controllably vary by changing the structure of the polymer chains. In contrast, the activation energy provides a framework to understand how chain architecture and packing might determine solute transport and thus provides a molecular framework for understanding transport in polymers.

In this work, we focus on this issue by utilizing temperature dependent polymer segmental dynamics towards understanding the key factors determining transport barriers in a polymer nanocomposite. In particular, we focus on melts of polymer chain grafted inorganic spherical silica nanoparticles (polymer grafted nanoparticles, GNP). It is well known that the structure of densely grafted polymer brushes depends on several factors such as the grafting density, polymer chain length, and the core size.[8-10] The conformation of a polymer brush on a single spherical GNP varies with distance from the NP surface as the space available to the polymer segments increases with increasing distance, leading to less chain crowding. For melts of GNPs, i.e., a system comprised of only GNPs with no added solvent, we additionally have to consider how the brushes on adjacent

GNPs interact and pack.[11,12]. These ideas have been built into a series of models,[13, 14] which all imply a transition between a dry brush regime with highly stretched polymer chain fragments to a interpenetrated polymer brush where the chains assume their melt-like state (assumed by chains that are not tethered to surfaces) as a function of increasing distance.[14] Wei et al.[15] showed that these regions are distinct dynamically as well, with the local dynamics being slower closer to the surface, presumably due to the steric effects of the neighboring brushes and the grafting surface. Thus, the structure and the dynamics of the polymer are controllable by varying the parameters defining these GNPs.

These structural changes are conjectured to be important since one-component melts of GNP have unusual transport properties: for example, gas permeability goes through a maximum as a function of polymer chain length (the maximum occurs at a molecular weight M_n ~ 90 kDa at 308 K, with grafting density of ρ_g ~ 0.47 chains/nm^2 , on silica cores with radius R_c = 7 nm in the case of poly(methyl acrylate), PMA, grafts), with this maximum being about an order of magnitude larger than that of the neat polymer[16]. While measured free volume element sizes in the GNPs, as measured by PALS, are larger than that of neat polymer, the density of the polymer phase remains nearly the same in the GNPs[16] compared to the melt[17]. Our previous work,[18] using quasielastic neutron scattering (QENS), showed that the data are well-described by the anomalous jump diffusion model where both the characteristic time scale, τ_0, and jump lengths, ℓ_o, depend on graft chain length, from which we obtained an apparent diffusion coefficient, $D = \ell_0^2/\tau_0$. Note that this diffusion coefficient is in a time regime where the segments execute hop-like motions – thus this is not a true diffusion coefficient which characterizes the long-time random motion of the segments. However, past work on substituted polyacetylenes show that such high frequency

motion correlated well with the measured gas permeabilities[19] – hence, while there are caveats, these "diffusion coefficients" have value in this exercise. This paper goes beyond previous observations of speeded up local polymer dynamics, and their empirical relationship to gas permeability and constructs the molecular basis of these results.

To this end, we critically examine the temperature dependence of both ℓ_o and τ_0. We find that while ℓ_o is essentially temperature independent for each system (but different for the different graft lengths), the activation energy obtained from the temperature dependence of the relaxation times (τ_0) shows a minimum at roughly the chain length where the chains are the most stretched. We propose that this behavior of the activation energy and ℓ_o, in particular its unusual behavior with increasing chain length, are direct reflections of brush structural transition from one comprised of stretched chains to interpenetrated polymers. This provides an underlying physical picture as to why the diffusivity of light gases in GNP show the unexpected experimental trends.

Materials and Methods: We utilize spherical SiO_2 NPs (14±4 nm diameter, Nissan) with PMA grafts[20] (see SI), where both the molecular weight (M_n ~ 29 to 136 kDa, DI~1.05-1.25) and grafting density ($\rho_g \sim$ 0.11, 0.47 and 0.66 chains/nm^2) were systematically varied. To understand the origin of the scattering intensity we list the scattering cross sections, which are a measure of the scattering probability of the different components. The large incoherent scattering cross section of hydrogenated PMA [$\sigma_{inc,PMA} \sim 4.439\ cm^{-1}$] compared to the coherent scattering cross section of hydrogenated PMA [$\sigma_{coh,PMA} \sim 0.022\ cm^{-1}$] and the total scattering cross section of SiO_2 [$\sigma_{tot} = \sigma_{inc} + \sigma_{coh};\ \sigma_{tot,SiO_2} \sim 0.224\ cm^{-1}$] ensures that >92 % of the quasielastic neutron scattering observed from the composites are related to the self-motion of the hydrogen atoms on the graft

polymer chains – this is augmented by the fact that the silica content is always less than 15 vol%. As both the main chain and the ester side groups are hydrogenated, the measured dynamics are a combination of the relaxations from both moieties.

QENS measurements were carried out on three different spectrometers – the High Flux Backscattering Spectrometer (HFBS, q ~ 2 – 15 nm^{-1})[21] at the NIST Center for Neutron Research (NCNR), SPHERES[22] (q ~ 3 – 17 nm^{-1}) operated by JCNS at the Heinz Maier-Leibnitz Zentrum (MLZ) and on IRIS[23] (q ~ 5 – 18 nm^{-1}) at the ISIS Neutron and Muon Source. The wavevector q is dependent on the incoming wavelength of the neutron beam and the scattering angle θ ($q = \frac{4\pi}{\lambda}\sin\left(\frac{\theta}{2}\right)$). For inelastic and quasielastic scattering experiments this expression is a valid approximation as the change in energy of the neutrons (~ μeV) is much smaller than the energy of the incoming neutrons (~meV) and thus λ remains relatively the same. The wavevector is also inversely related to a corresponding real space length scale as $q \sim 2\pi/d$, where d is the corresponding length scale for a particular q value. The accessible temporal range for the instruments is different (HFBS, t < 2500 ps; SPHERES, t < 3000 ps; IRIS, t < 150 ps) and due to this the range of temperatures studied are different. On HFBS and SPHERES, we employed 358 - 420K, while on IRIS it is 400 – 445 K. As the nominal calorimetric glass transition temperature (T_g) of PMA is ~ 290 K, we are always well above $1.2T_g$; thus, these systems are above the temperature where dynamic heterogeneities seen in glass forming liquids manifest themselves. For calculating intermediate scattering functions, the instrumental resolution function was measured at 4K on HFBS and SPHERES and 10K on IRIS, the temperature where most dynamic processes are expected to be frozen, for one sample and subsequently used to normalize all samples measured on the same instrument. To account for the differences in neutron transmission across different

GNP films, the maximum value of S(q,ω) in high temperature data and the resolution function were scaled to 1 (See SI, Eq. S1, S2) . To ensure data consistency, data at similar nominal temperatures were compared across different spectrometers with similar resolution (HFBS and SPHERES) as well as different resolutions (HFBS and IRIS). The elastic scans suggested that the effective T_g (beyond which dynamics associated with the α-relaxation are accessed by QENS) was around ~310 K on HFBS and SPHERES. As IRIS accesses time scales smaller than what can be accessed on HFBS and SPHERES, only spectra at higher temperatures was collected on IRIS. All data was subject to a background subtraction to remove the contributions from the sample holder as well as corrected for detector efficiencies using a reference vanadium sample. Since all samples had a neutron transmission of 90% or greater, there was no need for multiple scattering corrections. Data were reduced and analyzed using combinations of DAVE[24], SLAW[25] and MANTID[26].

Results and Discussion: Figure 1(A) shows the temperature dependence of the raw QENS spectra at a single wavevector, q = 11.1 nm^{-1} for a representative GNP with M_n = 88 kDa ($\rho_g \sim$ 0.47 chains/nm^2). With increasing temperature, the QENS spectra broaden indicating that more of the system dynamics occurs within the instrumental time window. The data were Fourier transformed into the time domain and divided by the instrumental resolution function to obtain intermediate scattering functions, I(q,t), Figure 1(B) (points). Each curve is first fit to a stretched exponential function: $I(q,t) = A(q,T) * \exp\left(-\left(\frac{t}{\tau_{KWW}(q,T)}\right)^{\beta(T)}\right) + C$, where β is a temperature dependent stretching parameter; A(T) and $\tau_{KWW}(q,T)$ are dependent on both the wavevector and temperature (lines in Figure 1B) and due to data normalization, A(q,T) ~ 1 for all the spectra considered in this work. C represents a contribution from atoms that are immobile within the instrument's timescale, and was estimated based on the decay of the correlation curves at large q values (small length

scales) previously[18]. The curves at different temperatures were shifted horizontally, Figure 1(C) and 1(D), to produce master curves for each sample. This validates the applicability of the empirical time-temperature superposition principle which is based on the assumption of a single process controlling dynamics across these length and time scales.

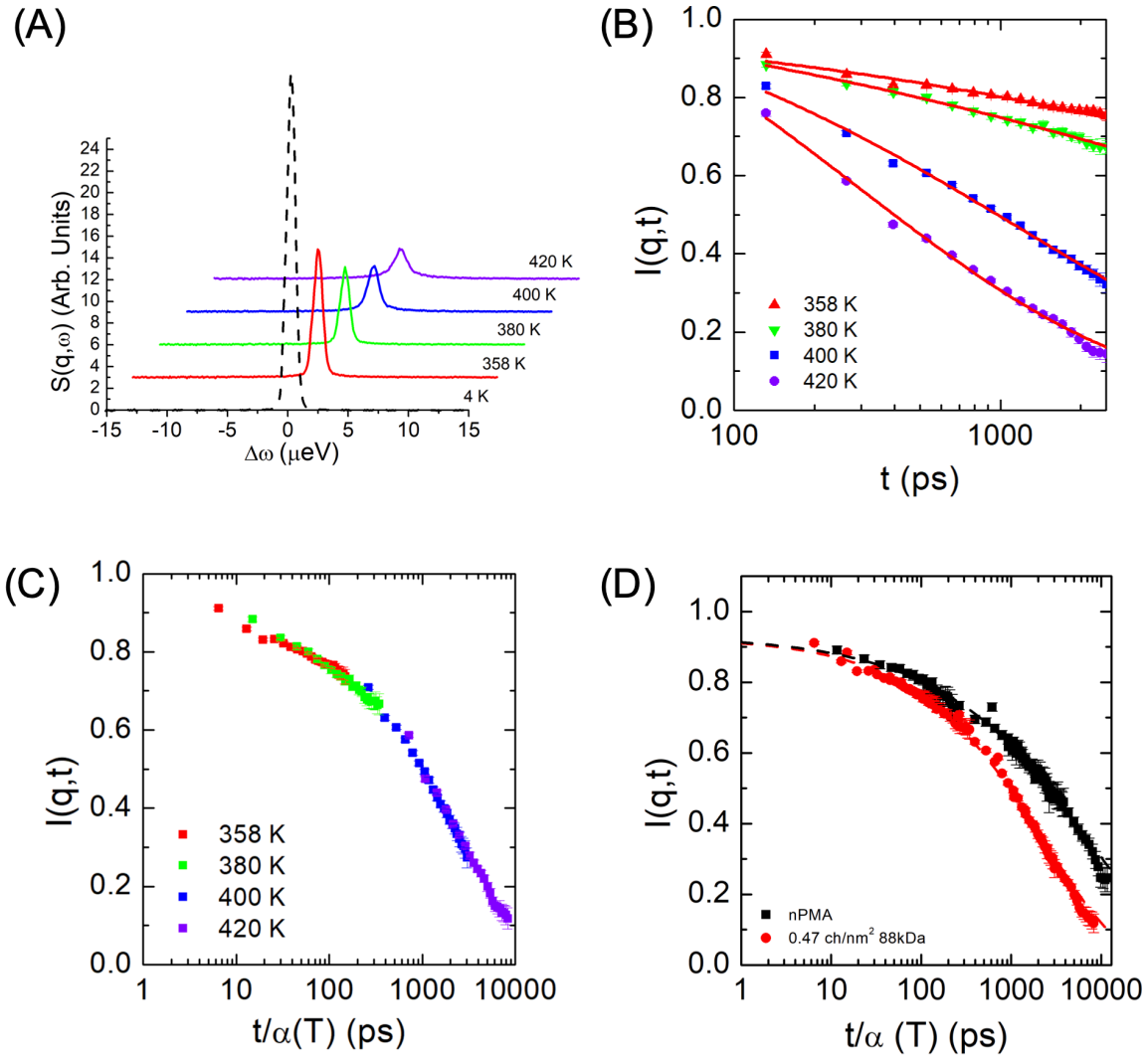

Figure 1. (A) Representative QENS spectra at a single wavevector, q =11.1 nm^{-1}, for a composite system with M_n = 88 kDa and $\rho_g \approx 0.47$ chains/nm^2 at different temperatures. The spectra are shifted for clarity. The corresponding instrumental resolution (Black line) is shown for reference.

(B) Intermediate scattering functions derived from the curves in subpart (A) for the 4 different temperatures. Red lines are fits using a stretched exponential function. (C) Superposed intermediate scattering functions at different temperatures and the same q-values shifted using an *ad hoc* shift factor (0.47 chains/nm^2 – 88 kDa, q = 11.1 nm^{-1}). The reference temperature is T_{ref} = 400 K. (D) Comparison between the shifted curves of the neat homopolymer (■) and the data in part C (■) at T_{ref} = 400 K. The lines are fits with a stretched exponential function with β = 0.44 for nPMA and 0.47 for the GNP.

We use this fact, along with the anomalous jump diffusion model,[27, 28] to extract jump time scales (τ_0) and a characteristic jump length (ℓ_0):

$$\tau_{KWW}(q) = \tau_0 \left(1 + \frac{1}{q^2 \ell_0^2}\right)^{\frac{1}{\beta}} \quad (2)$$

To a first approximation, the superposition of the curves in Figure 2(A) (α_T is the ad-hoc vertical shift factor which collapses the data at different temperatures) implies that the characteristic dynamic length scale associated with the system (ℓ_0) is essentially temperature independent and only the τ are temperature dependent. This assumption is validated by fitting the dispersion with the jump diffusion model; the effective jump length remains constant for all the temperatures studied [Figure 2(B)] as has also been found for a variety of other polymer melts[28, 29]. For the GNPs, only specimens with chain molecular weight between 80-100 kDa have ℓ_0 different from the neat homopolymer, and the length scale for M_n = 88 kDa (which corresponds to the most permeable material) is about 40% higher. Similar trends are found for each of the composites studied (See SI for high ρ_g data; Figures S1, S2). From a free volume element perspective, there is equivalence between the trends observed from PALS experiments on these materials[16] and the trends in the jump length, suggesting a possible correlation between the two quantities. From a

physical standpoint, this makes sense due to the fact that larger fluctuations could lead to temporally larger "free volume" elements even though the overall density would remain constant at all times consistent with the previous experimental results[16]. The temporal nature arises from the fact that the relaxation of the chains would lead to changes in local density, observations of which will be dependent on the time scale of the fluctuations. If the motion of the chains are much slower than the observation timescale, the density fluctuations are "frozen" in place and information related to these fluctuations will not be probed in the measurement. On the other hand, if the time scale of the fluctuations are similar to the probe used, the effect of these fluctuations must be explicit in the measurement. The effect of the fluctuations are extremely localized and their effect on the density is minimal as the density averages overall many different events occurring in the polymer. Analogous simulations have also shown that the transverse fluctuations of polymer brushes are dependent on chain length and distance of the segments from the surface of the NP[12].

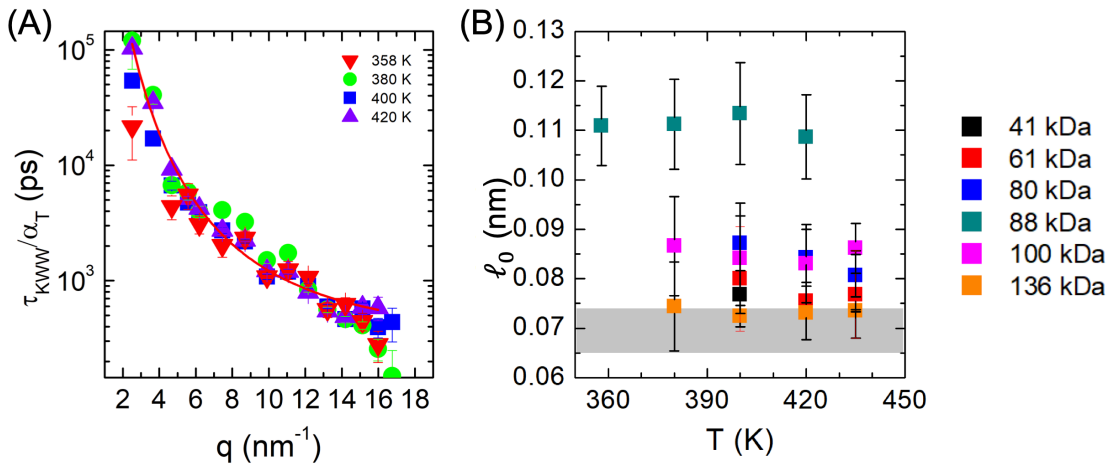

Figure 2. (A) Superposed master relaxation time dispersion for a composite system with graft M_n = 88 kDa for different wavevectors. The reference temperature for the shifted data is 400 K. Data

were collected on HFBS. Red line is a fit to the anomalous jump diffusion model using the parameters calculated for T = 400 K. (B) Calculated jump lengths from best fits to the dispersion of relaxation times for different graft molecular weights ($\rho_g \approx 0.47$ chains/nm^2) at different temperatures. The grey band represents the jump length values for the neat homopolymer with no NPs.

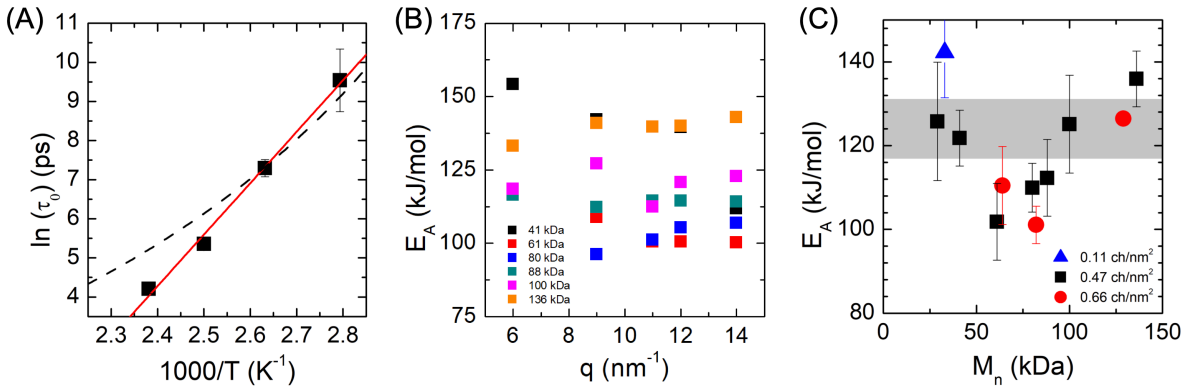

Figure 3. (A) Natural logarithm of the characteristic times related to jumps calculated using the anomalous jump diffusion model at different temperatures. Red line is the fit to the Arrhenius equation and the dashed black line corresponds to the WLF-like relaxation for PMA based GNPs. (B) Calculated activation energies at different wavevectors for composites with different graft molecular weights. The activation energies are essentially independent of wavevector. (C) Activation energies calculated using the jump diffusion model at different graft molecular weights and grafting densities (▲ – 0.11, ■ – 0.47, ● – 0.66 chains/nm^2). A clear minimum is observed at an intermediate molecular weight. The grey band represents the activation energy of the neat homopolymer with no NPs.

The observed temperature dependence of the τ is much stronger than that obtained from Williams-Landell-Ferry (WLF) fits to rheological data (these parameters remain constant for all different

GNPs and PMA homopolymers irrespective of changes in chain molecular weight or grafting density) at lower temperatures (293 – 358 K) for the same GNPs as used in this study[16], and an Arrhenius-like behavior is observed [Figure 3(A)]. We fit each of the curves to the Arrhenius model, $\tau = \tau_\infty \exp\left(\frac{E_A}{RT}\right)$ and extract the activation energies, E_A, for different graft molecular weights and grafting densities. We also compute E_A at different wavevectors using the definition of the mean relaxation time for a stretched exponential function $< \tau > = \frac{\tau_{KWW}\Gamma\left(\frac{1}{\beta}\right)}{\beta}$. As seen in Figure 3(B), the activation energy derived in this manner is essentially q independent for the different graft molecular weights at $\rho_g \sim$ 0.47 chains/nm^2 (See SI for higher ρ_g, Figure S2) and closely matches the trends and absolute values of activation energies obtained from the jump diffusion model, Figure 3(C).

The most striking takeaway from these results is the graft molecular weight dependent E_A has an apparent minimum in the 50-75 kDa range of graft chain molecular weights. Generally, for polymeric materials, the temperature response is a function of its chemical structure and packing, but essentially independent of chain length especially in this range. For confined systems, which represent one extreme of packing, such as highly loaded polyethylene-alt-propylene composites[30], and poly(ethylene oxide) in nanoporous media[31], no change in E_A was found. For GNP melts, the WLF parameters have also been reported to be independent of grafting density and molecular weights[16, 32], thus making such a minimum more surprising. The lowering of the E_A is also observed at a higher grafting density ($\rho_g \sim$ 0.66 chains/nm^2).

To explain these observations, we first consider recent theoretical work by Midya et al.[12], which suggests that the height of the grafted polymer brush, h, in a GNP melt can be obtained following space filling arguments, namely $\frac{4}{3}\pi(R_c + h)^3 = \frac{4}{3}\pi R_c^3 + 4\pi R_c^2 \rho_g \frac{N}{\rho}$, where N, b, ρ are the number of Kuhn monomers per grafted chain, the Kuhn length and the Kuhn monomer density of the chains, respectively[33]. A key assumption here is that there is no variation of the polymer density for all graft chain lengths, and thus the total "unoccupied" volume is likely not very different from the reference melt state; this assumption has previously been verified by density measurements from an analogous sample set[16].

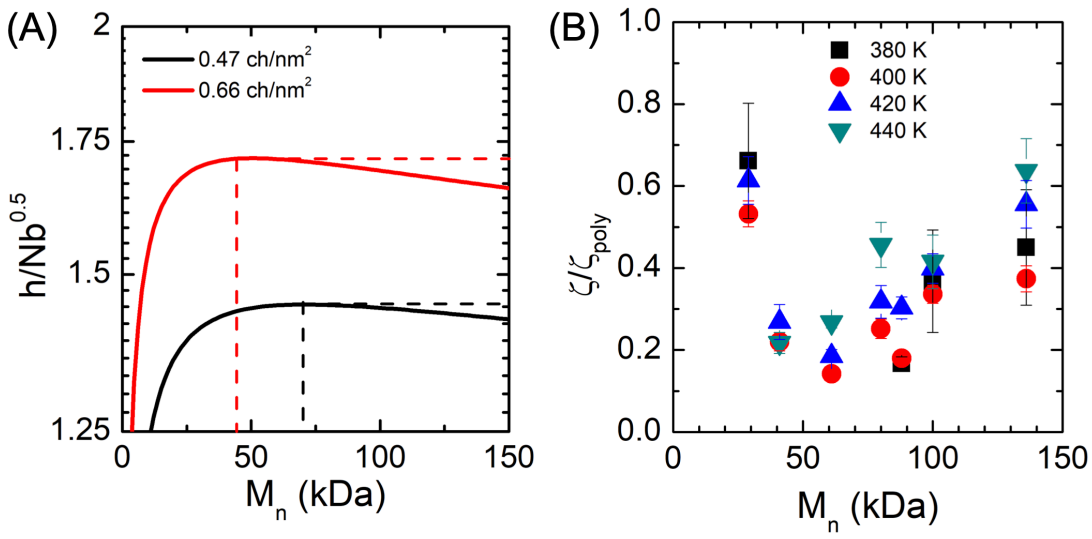

Figure 4: (A) Degree of stretching based on the space filling model of Midya et al. [12] for $\rho_g \sim 0.47$ ch/nm^2 (-) and 0.66 ch/nm^2 (-). The lines reflect numbers based on theoretical derivations rather than experimental results. (B) Normalized friction coefficients based on the calculated diffusion coefficients ($D = \ell_0^2/6\tau_0$; $\zeta = k_BT/D$) for $\rho_g \sim 0.47$ ch/nm^2 at different temperatures.

From this expression we can estimate the mean chain stretching free energy in the GNP layers[34] as $\Delta F \sim k_B T \frac{3}{2}\left(\frac{h}{b\sqrt{N}}\right)^2$. This quantity varies non-monotonically as a function of N at fixed ρ_g (Figure 4(A)), and for $\rho_g \sim 0.47$ chains/nm^2, it is predicted to be maximum for $M_n \sim 70$ kDa, while for $\rho_g \sim 0.66$ chains/nm^2, it occurs at ~50 kDa. Our previous work has shown that there are changes in the characteristic correlation length scale as a function of graft chain length, highlighted by changes in crossover of the relaxation times between two asymptotic scaling laws of $q^{-2/\beta}$ and q^{-2} (See SI, Figure S4)[18, 35]. Given that this might reflect a length scale at which chain connectivity related motion becomes important[36], the increasing crossover length scale for the grafted chains (lower q_c values) also lends credence to the fact that extension changes with graft chain length. We observe that the prediction of maximum stretching for the lower ρ_g closely corresponds to the location of the minimum in E_A; our limited data for the higher ρ_g preclude a definitive conclusion.

We now seek to understand the minimum activation energy as a function of chain molecular weight. The (local) segmental dynamics of a polymer chain are well described by an overdamped Langevin equation so that the time constant for local motion follows: $\tau \sim \zeta/k_{poly}$, with a characteristic spring constant, k_{poly} and local friction coefficient, ζ. Even though the grafted chains are extended relative to their ungrafted counterparts [Figure 4(A)], the chain extension is typically small, such that they are still Gaussian-like and can be described by the same spring constant ($k_{poly} \sim k_BT/b^2$; changes in the Kuhn length, b, are likely small) as a polymer melt. Thus, we conclude that changes in spring constant are not the primary source of the activation energy minimum. The primary factor which leads to the reduction in relaxation times is thus the segmental friction experienced by the chains. Although the calculations use the average degree of extension to match the ensemble averaged dynamics measured through QENS, simulations have shown that the degree

of extension is dependent on the radial distance from the surface[12]. The segmental friction can be readily estimated from the effective segmental diffusion coefficient, $\zeta = k_BT/D_{poly}$ ($D_{poly} = <\ell>^2/6\tau$) [Figure 4(B); See SI for trends from elastic scans on the same materials, Figure S5]. This results asserts the primary role of the reduced friction coefficient [which is 5x lower at the minimum, Figure 4(B)].

Experiments[37] and simulations[38] have shown that extended chains have a decreased effective monomeric friction coefficients relative to their bulk, Gaussian counterparts, though the decrease depends on the chain architecture and the tension. Bobbili and Milner[38] noted that even small values of tension ($f \sim k_BT/b$), which are approximately equivalent to the amount of tension in these graft chains, lead to a ~2x drop in the friction coefficient. Since we see a ~5x drop in the most extreme case, this chain extension argument only provides a partial explanation. While the measurement of the chain stretching and how it affects local friction is thus a critical, open question that is outside the purview of the current paper, it nevertheless is clear that the bigger effect it has is on friction and not on the local elasticity.

Rheologically, we know that the systems with short chains, with $M_n < 80$ kDa behave akin to soft, jammed solids[16]. In these jammed solids, the brush chains on adjacent NPs hardly interpenetrate, but beyond $M_n \sim 80$ kDa the brushes on adjacent NPs can interpenetrate much more readily. For molecular weights below this crossover, the brush chains, which are required to fill space, are extended as well as frustrated leading to inefficient "packing". The packing we refer to is akin to the packing of hard spheres at different volume fractions – analogous to the ECNLE theory proposed by Mirigian and Schweizer[39, 40]. A larger jump length of the graft segments coupled with

the reduced friction coefficient implies that the compressibility of the graft polymer phase is higher when compared to the homopolymer melt ($\delta V/V^2 \sim k_B T \kappa_T$; $\delta V_{graft} > \delta V_{poly}$). This results in (from an equivalence viewpoint) a lower hard sphere volume fraction of the polymer phase near the maximum in the gas permeability (Mn ~ 88 kDa; jump length was 60% higher [Figure 2(B)]) observed in these constructs.

These conclusions are also consistent with the lowering of activation energies observed in these systems, as the importance of chain packing in determining activation barriers was also put forth much earlier by Bershtein[41], based on empirical observations. This, thus, provides the second piece which can explain the larger than expected decrease in the friction coefficients in the vicinity of the maximum chain stretching. On increasing the molecular weight, as the graft chains interpenetrate, following the arguments of Bockstaller and coworkers[9, 42], the polymer phase behaves more akin to a melt and the activation energy and friction coefficients increase. This is supported by the corresponding decrease in the effective segment jump length, Figure 2(B). While these qualitative ideas are in agreement with other experiments and previous work[42, 43], there is no fully quantitative model that captures this physics. There is significant correlation between the three quantities – the accelerated segmental dynamics, the stretching of the brush and the lowering of activation energy, and while it is difficult to pinpoint the key driving force, they are intrinsically linked to each other and the structure of the polymer brush. Based on the expected changes in chain extension with molecular weight due to the additional steric crowding at higher grafting densities, as shown in Figure 4(A), we would expect the minimum in apparent activation energy to be grafting density dependent. From the limited data we have at the higher grafting density, we do

observe lower apparent activation energies for M_n ~ 64 kDa and 82 kDa, but whether they portray a true minimum in the activation energy remains an open question.

A second important point is the effect of the different mobilities of the dry inner brush vs the interpenetrated outer brush layer. This effect of the brush microstructure would likely lead to different mobilities at different point along the chain moving away from the surface which might influence the stretching factors and the intrinsic non-exponentiality of the dynamics in a way which is unknown. Our work probes the average dynamics from the entire chain, without any distinction between the inner extended layer and outer interpenetrated layer. Previous work for dilute solutions of GNPs have shown that both layers follow Zimm dynamics with different relaxation times and this suggests that stearic hinderance induced changes might have the same non-exponential dynamics with different relaxation times[15]. More detailed studies in GNPs with appropriately labeled chains are required to systematically study the differences in mobility between the two layers.

Lastly, we focus on the relevance of these results on the transport of penetrants in polymers and GNP based membranes. The importance of thermal motion has been shown through coarse-grained molecular dynamics simulations, where Debye-Waller vibrations are important drivers for diffusion for penetrants larger than a critical size[3]. Similarly, theoretical approaches have illustrated the intimate relationship between the α-relaxation and penetrant hopping[44]. As we noted previously, the transport of penetrants through polymer membranes, the diffusion constant is an activated process dependent on the penetrant diameter, Eq. (1). In our language, penetrants with sizes smaller than ℓ_0 would face no penalty while the prefactor c in the Brandt/Freeman expression

has a frictional origin. Thus, for GNPs, the change in chain extension and packing, and how this affects local friction, would manifest itself in a change in these apparent metrics (c and f) and explain how the macroscopic transport activation energies will likely vary.

Conclusion: Grafting polymers to the curved surface of a NP has been shown to enhance penetrant diffusivity, a phenomenon that is strongly dependent on the graft chain length at a fixed NP size and grafting density. The key dynamic driving force for faster diffusivity is shown here to be related to the fact that the characteristic time constant, relaxation length scale (Ref 15 and this work) and activation energy display unusual dependences on graft length and grafting density. Based on these results, we propose that the mechanism that controls behavior is a transition in brush structure evolving from "dry" to "interpenetrated" with increasing chain length. For low graft molecular weights, the degree of extension of the chains increases with increasing molecular weight up to a certain molecular weight. This results in disrupted chain packing and reduced barriers to motion. Beyond a certain critical molecular weight (~88 kDa for this set of GNPs , ρ_g ~ 0.47 ch/nm^2), the chains become more melt like and the activation energy recovers to the level of the reference melt. Our results therefore highlight the critical importance of this structural transition in determining gas transport and presumably other dynamic properties in these novel constructs.

ASSOCIATED CONTENT

Supporting Information – The Supporting Information is available free of charge on the ACS publications website.

Synthetic details of the GNPs, description of general sample preparation protocol and experimental details, additional experimental data for other grafting densities, theoretical basis for brush stretching, volume fluctuations argument for varying volume fraction of hard spheres.

AUTHOR INFORMATION

Corresponding Author

*Email:sk2794@columbia.edu

ACKNOWLEDGMENTS

Financial support for this research was provided by the Department of Energy under grant DE-SC0021272. Access to HFBS was provided by the Center for High Resolution Neutron Scattering, a partnership between the National Institute of Standards and Technology and the National Science Foundation under Agreement No. DMR-1508249. Data collected on IRIS was through proposals RB1810435[45] and RB1910201[46]. We would like to thank Alejandro Krauskopf, Sophia Chan and Marshall Tekell for experimental assistance. The identification of any commercial product or trade name does not imply endorsement or recommendation by the National Institute of Standards and Technologies.

REFERENCES

1. Brandt, W. W., Model Calculation of the Temperature Dependence of Small Molecule Diffusion in High Polymers. *J Phys Chem-Us* **1959,** *63* (7), 1080-1084.
2. Freeman, B. D., Basis of permeability/selectivity tradeoff relations in polymeric gas separation membranes. *Macromolecules* **1999,** *32* (2), 375-380.
3. Meng, D.; Zhang, K.; Kumar, S. K., Size-dependent penetrant diffusion in polymer glasses. *Soft Matter* **2018,** *14* (21), 4226-4230.
4. Thran, A.; Kroll, G.; Faupel, F., Correlation between fractional free volume and diffusivity of gas molecules in classy polymers. *J Polym Sci Pol Phys* **1999,** *37* (23), 3344-3358.
5. Park, J. Y.; Paul, D. R., Correlation and prediction of gas permeability in glassy polymer membrane materials via a modified free volume based group contribution method. *Journal of Membrane Science* **1997,** *125* (1), 23-39.
6. Costello, L. M.; Koros, W. J., Effect of structure on the temperature dependence of gas transport and sorption in a series of polycarbonates. *Journal of Polymer Science Part B: Polymer Physics* **1994,** *32* (4), 701-713.
7. Rowe, B. W.; Robeson, L. M.; Freeman, B. D.; Paul, D. R., Influence of temperature on the upper bound: Theoretical considerations and comparison with experimental results. *Journal of Membrane Science* **2010,** *360* (1-2), 58-69.
8. Choi, J.; Hui, C. M.; Schmitt, M.; Pietrasik, J.; Margel, S.; Matyjazsewski, K.; Bockstaller, M. R., Effect of polymer-graft modification on the order formation in particle assembly structures. *Langmuir* **2013,** *29* (21), 6452-9.
9. Choi, J.; Hui, C. M.; Pietrasik, J.; Dong, H. C.; Matyjaszewski, K.; Bockstaller, M. R., Toughening fragile matter: mechanical properties of particle solids assembled from polymer-grafted hybrid particles synthesized by ATRP. *Soft Matter* **2012,** *8* (15), 4072-4082.
10. Mark, C.; Holderer, O.; Allgaier, J.; Hubner, E.; Pyckhout-Hintzen, W.; Zamponi, M.; Radulescu, A.; Feoktystov, A.; Monkenbusch, M.; Jalarvo, N.; Richter, D., Polymer Chain Conformation and Dynamical Confinement in a Model One-Component Nanocomposite. *Phys Rev Lett* **2017,** *119* (4).
11. Kapnistos, M.; Semenov, A. N.; Vlassopoulos, D.; Roovers, J., Viscoelastic response of hyperstar polymers in the linear regime. *J Chem Phys* **1999,** *111* (4), 1753-1759.
12. Midya, J.; Rubinstein, M.; Kumar, S. K.; Nikoubashman, A., Structure of Polymer-Grafted Nanoparticle Melts. *Acs Nano* **2020**.
13. Daoud, M.; Cotton, J. P., Star Shaped Polymers - a Model for the Conformation and Its Concentration-Dependence. *J Phys-Paris* **1982,** *43* (3), 531-538.
14. Ohno, K.; Morinaga, T.; Takeno, S.; Tsujii, Y.; Fukuda, T., Suspensions of silica particles grafted with concentrated polymer brush: Effects of graft chain length on brush layer thickness and colloidal crystallization. *Macromolecules* **2007,** *40* (25), 9143-9150.
15. Wei, Y.; Xu, Y. F.; Faraone, A.; Hore, M. J. A., Local Structure and Relaxation Dynamics in the Brush of Polymer-Grafted Silica Nanoparticles. *Acs Macro Letters* **2018,** *7* (6), 699-704.
16. Bilchak, C. R.; Buenning, E.; Asai, M.; Zhang, K.; Duming, C. J.; Kumar, S. K.; Huang, Y. C.; Benicewicz, B. C.; Gidley, D. W.; Cheng, S. W.; Sokolov, A. P.; Minelli, M.; Doghieri, F., Polymer-Grafted Nanoparticle Membranes with Controllable Free Volume. *Macromolecules* **2017,** *50* (18), 7111-7120.

17. Holt, A. P.; Roland, C. M., Segmental and secondary dynamics of nanoparticle-grafted oligomers. *Soft Matter* **2018,** *14* (42), 8604-8611.
18. Jhalaria, M.; Buenning, E.; Huang, Y.; Tyagi, M.; Zorn, R.; Zamponi, M.; Garcia-Sakai, V.; Jestin, J.; Benicewicz, B. C.; Kumar, S. K., Accelerated Local Dynamics in Matrix-Free Polymer Grafted Nanoparticles. *Phys Rev Lett* **2019,** *123* (15), 158003.
19. Kanaya, T.; Tsukushi, I.; Kaji, K.; Sakaguchi, T.; Kwak, G.; Masuda, T., Role of local dynamics in the gas permeability of glassy substituted polyacetylenes. A quasielastic neutron scattering study. *Macromolecules* **2002,** *35* (14), 5559-5564.
20. Li, C.; Benicewicz, B. C., Synthesis of well-defined polymer brushes grafted onto silica nanoparticles via surface reversible addition-fragmentation chain transfer polymerization. *Macromolecules* **2005,** *38* (14), 5929-5936.
21. Meyer, A.; Dimeo, R. M.; Gehring, P. M.; Neumann, D. A., The high-flux backscattering spectrometer at the NIST Center for Neutron Research. *Rev Sci Instrum* **2003,** *74* (5), 2759-2777.
22. Wuttke, J.; Budwig, A.; Drochner, M.; Kammerling, H.; Kayser, F. J.; Kleines, H.; Ossovyi, V.; Pardo, L. C.; Prager, M.; Richter, D.; Schneider, G. J.; Schneider, H.; Staringer, S., SPHERES, Julich's high-flux neutron backscattering spectrometer at FRM II. *Rev Sci Instrum* **2012,** *83* (7).
23. Carlile, C. J.; Adams, M. A., The Design of the Iris Inelastic Neutron Spectrometer and Improvements to Its Analyzers. *Physica B* **1992,** *182* (4), 431-440.
24. Azuah, R. T.; Kneller, L. R.; Qiu, Y. M.; Tregenna-Piggott, P. L. W.; Brown, C. M.; Copley, J. R. D.; Dimeo, R. M., DAVE: A Comprehensive Software Suite for the Reduction, Visualization, and Analysis of Low Energy Neutron Spectroscopic Data. *J Res Natl Inst Stan* **2009,** *114* (6), 341-358.
25. Wuttke, J. J. Wuttke. SLAW: Neutron scattering histograms to scattering law converter. http://apps.jcns.fz-juelich.de/slaw.
26. Arnold, O.; Bilheux, J. C.; Borreguero, J. M.; Buts, A.; Campbell, S. I.; Chapon, L.; Doucet, M.; Draper, N.; Leal, R. F.; Gigg, M. A.; Lynch, V. E.; Markvardsen, A.; Mikkelson, D. J.; Mikkelson, R. L.; Miller, R.; Palmen, K.; Parker, P.; Passos, G.; Perring, T. G.; Peterson, P. F.; Ren, S.; Reuter, M. A.; Savici, A. T.; Taylor, J. W.; Taylor, R. J.; Tolchenoy, R.; Zhou, W.; Zikoysky, J., Mantid-Data analysis and visualization package for neutron scattering and mu SR experiments. *Nucl Instrum Meth A* **2014,** *764*, 156-166.
27. Arbe, A.; Colmenero, J.; Alvarez, F.; Monkenbusch, M.; Richter, D.; Farago, B.; Frick, B., Non-Gaussian nature of the alpha relaxation of glass-forming polyisoprene. *Phys Rev Lett* **2002,** *89* (24).
28. Arbe, A.; Colmenero, J.; Alvarez, F.; Monkenbusch, M.; Richter, D.; Farago, B.; Frick, B., Experimental evidence by neutron scattering of a crossover from Gaussian to non-Gaussian behavior in the alpha relaxation of polyisoprene. *Phys Rev E* **2003,** *67* (5).
29. Capponi, S.; Arbe, A.; Cerveny, S.; Busselez, R.; Frick, B.; Embs, J. P.; Colmenero, J., Quasielastic neutron scattering study of hydrogen motions in an aqueous poly(vinyl methyl ether) solution. *J Chem Phys* **2011,** *134* (20).
30. Krutyeva, M.; Pasini, S.; Monkenbusch, M.; Allgaier, J.; Maiz, J.; Mijangos, C.; Hartmann-Azanza, B.; Steinhart, M.; Jalarvo, N.; Ivanova, O.; Holderer, O.; Radulescu, A.; Ohl, M.; Falus, P.; Unruh, T.; Richter, D., Polymer dynamics under cylindrical confinement featuring a locally repulsive surface: A quasielastic neutron scattering study (vol 146, 203306, 2017). *J Chem Phys* **2017,** *146* (20).

31. Krutyeva, M.; Martin, J.; Arbe, A.; Colmenero, J.; Mijangos, C.; Schneider, G. J.; Unruh, T.; Su, Y. X.; Richter, D., Neutron scattering study of the dynamics of a polymer melt under nanoscopic confinement. *J Chem Phys* **2009,** *131* (17).
32. Goel, V.; Pietrasik, J.; Matyjaszewski, K.; Krishnamoorti, R., Linear Viscoelasticity of Polymer Tethered Highly Grafted Nanoparticles. *Controlled/Living Radical Polymerization: Progress in Atrp* **2009,** *1023*, 257-+.
33. Semenov, A. N., Contribution to the Theory of Microphase Layering in Block-Copolymer Melts. *Zh Eksp Teor Fiz+* **1985,** *88* (4), 1242-1256.
34. Rubinstein, M.; Colby, R. H., *Polymer physics*. Repr. with corrections. ed.; Oxford University press: Oxford, 2016; p XI, 440 p.
35. Colmenero, J.; Arbe, A.; Alegria, A.; Monkenbusch, M.; Richter, D., On the origin of the non-exponential behaviour of the alpha-relaxation in glass-forming polymers: incoherent neutron scattering and dielectric relaxation results. *J Phys-Condens Mat* **1999,** *11* (10a), A363-A370.
36. Arbe, A.; Colmenero, J.; Monkenbusch, M.; Richter, D., Dynamics of glass-forming polymers: "Homogeneous" versus "heterogeneous" scenario. *Phys Rev Lett* **1998,** *81* (3), 590-593.
37. Ianniruberto, G.; Brasiello, A.; Marrucci, G., Simulations of fast shear flows of PS oligomers confirm monomeric friction reduction in fast elongational flows of monodisperse PS melts as indicated by rheooptical data. *Macromolecules* **2012,** *45* (19), 8058-8066.
38. Bobbili, S. V.; Milner, S. T., Chain tension reduces monomer friction in simulated polymer melts. *J Rheol* **2020,** *64* (6), 1373-1378.
39. Mirigian, S.; Schweizer, K. S., Elastically cooperative activated barrier hopping theory of relaxation in viscous fluids. II. Thermal liquids. *J Chem Phys* **2014,** *140* (19).
40. Mirigian, S.; Schweizer, K. S., Elastically cooperative activated barrier hopping theory of relaxation in viscous fluids. I. General formulation and application to hard sphere fluids. *J Chem Phys* **2014,** *140* (19).
41. Bershtein, V. A.; Egorov, V. M.; Emelyanov, Y. A.; Stepanov, V. A., The Nature of Beta-Relaxation in Polymers. *Polym Bull* **1983,** *9* (1-3), 98-105.
42. Lee, J.; Wang, Z.; Zhang, J.; Yan, J.; Deng, T.; Zhao, Y.; Matyjaszewski, K.; Bockstaller, M. R., Molecular Parameters Governing the Elastic Properties of Brush Particle Films. *Macromolecules* **2020,** *53* (4), 1502-1513.
43. Bilchak, C. R.; Huang, Y. C.; Benicewicz, B. C.; Durning, C. J.; Kumar, S. K., High-Frequency Mechanical Behavior of Pure Polymer-Grafted Nanoparticle Constructs. *Acs Macro Letters* **2019,** *8* (3), 294-298.
44. Zhang, R.; Schweizer, K. S., Correlated matrix-fluctuation-mediated activated transport of dilute penetrants in glass-forming liquids and suspensions. *J Chem Phys* **2017,** *146* (19).
45. Kumar, S. K.; Garcia Sakai, V.; Jhalaria, M. Study on the effect of polymer dynamics to the transport properties and macroscopic stiffening in polymer nanocomposites. data.isis.stfc.ac.uk/doi/STUDY/103197451/.
46. Kumar, S. K.; Garcia Sakai, V.; Jhalaria, M. Jump diffusion of small molecules in polymers □ influence of grafting on the mechanism of diffusion. data.isis.stfc.ac.uk/doi/STUDY/103219288/.